European Journal of Applied Sciences – Vol. 12, No. 2
Publication Date: April 25, 2024
DOI:10.14738/aivp.122.16797
Assem, H. D., Donkor, M. E. K., Tamakloe, R. Y., & Nkum, R. K. (2024). A Review of UV-Vis on Polymers; Polyaniline (PANI) and Its Nanocomposites. European Journal of Applied Sciences, Vol - 12(2). 322-346.
SERVICES FOR SCIENCE AND EDUCATION

A Review of UV-Vis on Polymers; Polyaniline (PANI) and Its Nanocomposites

Humphrey Darkeh Assem
Department of Physics Kwame Nkrumah University Science and Technology Kumasi-Ghana (West Africa)

Michael Edem Kweku Donkor
Department of Physics Kwame Nkrumah University Science and Technology Kumasi-Ghana (West Africa)

Reuben Yao Tamakloe
Department of Physics Kwame Nkrumah University Science and Technology Kumasi-Ghana (West Africa)

Robert K. Nkum
Department of Physics Kwame Nkrumah University Science and Technology Kumasi-Ghana (West Africa)

ABSTRACT

In recent years, the utilization of Polyaniline (PANI) and its nano-composites has garnered considerable attention across diverse domains encompassing electronics, sensing technologies, and energy storage applications due to their multifaceted utility. Central to the investigation of their properties is UV-Vis spectroscopy, which has emerged as an indispensable analytical tool. This review aims to shed light on recent advancements in UV-Vis spectroscopic techniques as applied to PANI films and their corresponding nano-composites. The discourse begins by explaining the fundamental principles of UV-Vis spectroscopy and its relevance in examining the electronic transitions within PANI and its nano-composites. Subsequently, the synthetic methodologies employed for fabricating PANI films and nano-composites are expounded upon, with particular emphasis on discerning the influence of various parameters on their optical attributes. Furthermore, the implications of dopants, oxidants, and nano structural configurations on the UV-Vis spectra of PANI are meticulously examined. Additionally, this review delves into the applications of UV-Vis spectroscopy in shedding more light on the structural and optical attributes of PANI-based materials tailored for specific functions such as chemical sensing, optoelectronics, and energy storage systems. Recent advancements in the development of innovative PANI nano-composites endowed with augmented optical properties are scrutinized, highlighting their potential utility across a spectrum of technological domains. Moreover, the challenges and prospective avenues in harnessing UV-Vis spectroscopy for the characterization of PANI films and nano-composites are deliberated upon, with strategies proposed to overcome limitations including spectral superposition, sample preparation intricacies, and the interpretation of complex spectra. Furthermore, prospective directions for

further research endeavours aimed at leveraging the full potential of UV-Vis spectroscopy in enhancing the comprehension and application scope of PANI-based materials are mapped out.

Keywords: Polyaniline (PANI), Nano-composites, UV-Vis spectroscopy, Spectroscopic techniques, Electronic transitions, Synthetic methodologies, Optical attributes, Dopants, Oxidants, Nano structural configurations, Structural attributes, Chemical sensing, Optoelectronics

HIGHLIGHTS

1. Polyaniline (PANI) and its nanocomposites exhibit versatility in applications spanning electronics, sensing technologies, and energy storage, underscoring their broad utility across diverse domains.
2. UV-VIS spectroscopy emerges as a pivotal analytical tool for scrutinizing the optical properties of PANI films, offering indispensable insights into their optical characteristics.
3. The fabrication techniques employed significantly impact the optical properties of PANI films and nanocomposites, highlighting the importance of method selection in tailoring their optical performance.
4. UV-VIS spectroscopy plays a crucial role in the comprehensive characterization of PANI materials, enabling a nuanced understanding essential for their effective utilization across varied applications.
5. Addressing challenges inherent in UV-Vis spectroscopy stands to enrich the understanding and application scope of PANI materials, necessitating the development of strategies to mitigate issues such as spectral superposition and complexities in sample preparation and interpretation.

INTRODUCTION

Polyaniline (PANI) has garnered significant attention across various disciplines due to its diverse electrical, optical, and chemical properties (Beygisangchin *et al.,* 2024; Banerjee, 2019). The application of PANI thin films and nano-composites in fields such as sensors, optoelectronic devices, and energy storage systems underscores the necessity of comprehending their optical behavior for improved functionality. UV-Vis spectroscopy emerges as a crucial analytical method for investigating these materials, providing deep insights into their electronic structure and interactions. PANI, as a member of conducting polymers, presents intriguing features stemming from the delocalization of π-electrons along its backbone, which can be manipulated through chemical doping or structural modifications (Ibanez *et al.* 2018). The fabrication of PANI thin films through techniques like spin-coating, dip-coating, or electrochemical deposition offers controlled environments for property exploration. UV-Vis spectroscopy, rooted in ultraviolet and visible light absorption, serves as a valuable tool for unraveling electronic transitions within PANI thin films, including π-π* transitions and charge transfer interactions. Analyzing absorption spectra aids in identifying characteristic peaks, facilitating deductions about structural and electronic alterations. Moreover, this academic review seeks to extensively explore UV-Vis spectroscopy, including its basic principles, complexities in instrumentation, wide-ranging applications, and inherent limitations, supported by relevant scholarly sources. The underlying principle of UV-Vis spectroscopy lies in the interaction

between matter and ultraviolet and visible light, resulting in electronic transitions and distinctive spectra, based on the energy disparity between ground and excited states (Förster, 2004; Penner, 2017). Moreover, nano-composites incorporating PANI exhibit enhanced properties compared to pristine polymer films, with UV-Vis characterization enabling the exploration of interactions between the polymer matrix and nanofillers, alongside the assessment of nanofiller morphology and concentration effects on optical properties.

Applications

UV-Vis spectroscopy finds applications in quantitative analysis, qualitative analysis, structural analysis, kinetic studies, DNA and protein analysis, and environmental monitoring (Harris, 2010; Pan et al., 2017). One common application is the determination of substance concentration using the Beer-Lambert law,

$$A = \varepsilon lc \quad ---------- (17)$$

where absorbance (A) is proportional to the molar absorptivity coefficient (ε), path length (b), and concentration (c). The technique is versatile, allowing the analysis of liquids, solids, and gases. UV–Vis–NIR spectrometer is able to monitor absorbance, A or transmittance, T in UV – Vis wavelength range. The relation between incident light of intensity, I and transmitted light of intensity I_0 and Transmittance, T is given by:

$$T = \frac{I}{I_0} \quad ---------- (18)$$

and transmission rate is given by:

$$(T\%) = \left(\frac{I}{I_0}\right)100\%$$

Absorbance, A is the inverse of transmittance, T and given by $log\frac{1}{T} = log\frac{I_0}{I}$

Thus,

$$A = -logT = \varepsilon lc \quad ---------- (19)$$

While absorbance displays a proportionality with sample concentration according to Beer's law and the optical path, transmittance is independent of sample concentration. Additionally, when the optical path is 1 cm and the concentration of the target substance is 1 mol/l, the phenomenon is referred to as molar absorption (Tolbin *et al.,* 2017). Molar absorption coefficient is a property of the substance that is typical under certain circumstances. The spectrometer can then be used to capture the UV-Vis spectrum.

UV-VIS SPECTROSCOPY IN MOLECULAR ANALYSIS

UV-Visible (UV-Vis) spectroscopy holds paramount significance in molecular analysis by concentrating on the intricate interplay between electromagnetic fields and matter. This analytical technique employs ultraviolet and visible light, inducing diverse electronic

transitions such as σ – σ*, n – σ*, n – π*, and π – π*, thereby affording valuable insights into distinct molecular orbitals (Zhao et al., 2020). The foundational principle of UV-Vis spectroscopy is grounded in the premise that chemical entities possess the capability to absorb ultraviolet or visible light, culminating in the generation of distinctive spectra. At the core of spectroscopy lies the essential interaction between light and matter. The creation of a spectrum ensues when matter undergoes light absorption through processes of excitation and de-excitation. Excitation occurs when electrons within the matter move from a ground state to an excited state upon absorption of ultraviolet radiation. The quantity of UV-Vis radiation assimilated by an electron corresponds to the energy difference, E, between its ground state and the excited state (Khan, 2019). This relationship is encapsulated by the expression:

$$\Delta E = E_1 - E_0 = h\nu = \frac{hc}{\lambda} - - - - - - - - - - (20)$$

The elevation of electrons to excited states or anti-bonding orbitals is a consequence of the absorption of incident UV-Vis radiation. For this transition to transpire, the photon energy must precisely align with the energy requisite for the promotion of an electron to the subsequent higher energy state. At the crux of this process lies the foundational concept of absorption spectroscopy. Three distinct categories of ground state orbitals play a pivotal role in the transition of electrons: n-atomic, π-molecular orbitals, and σ-molecular orbitals, alongside anti-bonding orbitals such as the π*- and σ*-orbitals (Sykes, 1986). A noteworthy instance of electronic transition involves the excitation of an electron from a σ-bonding orbital to a σ-anti-bonding orbital, denoted as a σ – σ* transition. Analogously, the π – π* transition signifies the excitation of an electron from a lone pair to an antibonding π orbital. Electronic transitions induced by the absorption of UV and visible light encompass σ – σ*, n – σ*, n – π*, and π – π*. The σ – σ* and n – σ* transitions entail higher energies, typically manifesting in the far UV region. Consequently, saturated groups exhibit limited absorption within the UV spectrum. Conversely, molecules featuring unsaturated centers undergo n – π* and π – π* transitions, characterized by lower energies and consequently manifesting at longer wavelengths than transitions to σ* anti-bonding orbitals.

UV-VIS SPECTROSCOPY FOR OBTAINING ANALYTICAL INFORMATION

UV-visible spectroscopic data holds significant utility in both qualitative and quantitative analyses of various compounds or molecules. Regardless of the specific analytical objective, it is imperative to employ a reference cell to nullify any potential influence from the solvent in which the compound is dissolved. For quantitative assessments, precise calibration of the instrument using known concentrations of the compound in a solution with identical solvent composition to that of the unknown sample becomes imperative. Conversely, if the aim is solely to ascertain the presence of a compound within the sample, the construction of a calibration curve may be deemed unnecessary (Blasco-Gomez, 2000). However, in scenarios such as degradation studies or reactions where the determination of compound concentration is pivotal, the establishment of a calibration curve becomes indispensable. Constructing a calibration curve necessitates the utilization of at least three concentrations of the compound, although employing five concentrations is preferred to enhance curve accuracy. These concentrations should span from slightly above the estimated concentration of the unknown sample to approximately an order of magnitude lower than the highest concentration (Smith,

2015). It is paramount that these calibration solutions be meticulously prepared using digital pipettes and volumetric flasks instead of less precise implements like graduated cylinders and beakers. Additionally, the calibration solutions should be evenly spaced apart to ensure a robust calibration curve.

Limitations

While UV-Vis spectroscopy finds extensive utility, it is not without inherent limitations. The technique offers constrained insights into particular functional groups, and the presence of absorbing species from external sources can introduce inaccuracies in the obtained results. Inadequate sensitivity may pose challenges in detecting low concentrations, and the opaqueness of certain samples may necessitate the application of specialized analytical methods (Hanson, 1995).

UV-Vis-NIR Spectrophotometer

The UV-Vis-NIR spectrophotometer is designed for the measurement of light absorbance or transmittance across the ultraviolet-visible (UV-Vis) wavelength range in a given medium. It encompasses essential components including UV and visible light sources, such as deuterium or hydrogen lamps and tungsten/halogen lamps respectively, alongside a monochromator, sample holder in the form of cuvettes, a detector, and a display interface. This instrumentation facilitates the examination of samples in various states, thereby furnishing invaluable data for a comprehensive UV-Vis spectrum as depicted in Figure 1. Upon exposure to incident light, an object experiences fundamental optical phenomena such as absorption, reflection, or transmission. The spectrophotometer serves as a pivotal tool for quantifying the extent of light absorption within the UV and Vis spectra. It gauges the intensity of light transmitted through the sample, contrasting it against a baseline measurement derived from the incident light source. Through the application of the Beer-Lambert Law, which delineates a direct correlation between the concentration of a substance in a sample, the path length traversed by light, and the resultant light absorption, the spectrophotometer is proficient in determining the concentration of specific analytes present within the sample (Purcell, 2013).

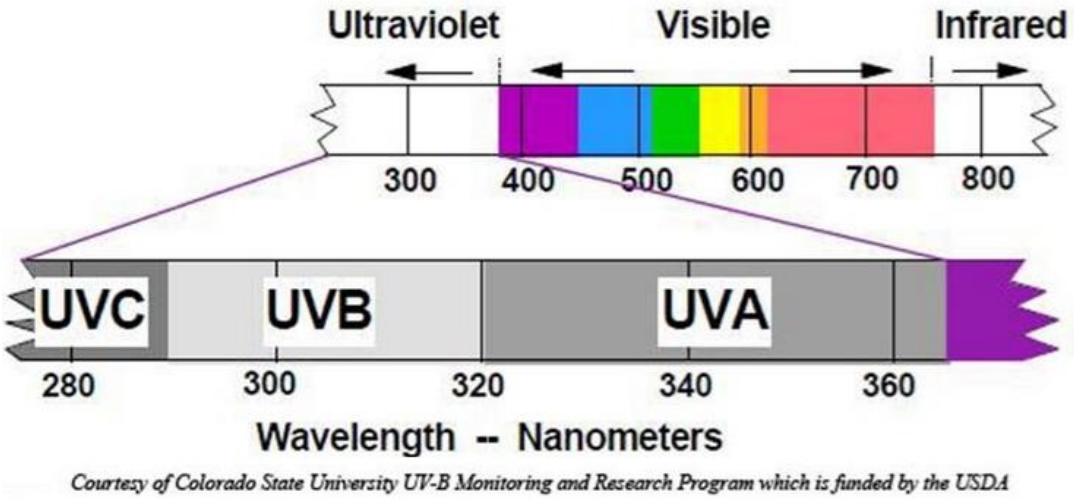


Figure 1: UV-Vis spectrum

INSTRUMENTATION FRAMEWORK: PARTS AND FUNCTION OF THE UV-VIS SPECTROPHOTOMETER

A conventional UV-Vis spectrophotometer constitutes essential elements, including a light source, monochromator, sample holder, detector, and data processor. The light source emits a continuous spectrum encompassing ultraviolet (UV) and visible (Vis) light wavelengths, while the monochromator selectively isolates precise wavelengths for analysis. Upon interaction with the sample, directed light undergoes transmission or reflection, and the resulting signal is captured by the detector (Skoog *et al.,* 2018). Subsequently, the acquired data undergoes processing to generate absorption or transmission spectra, facilitating comprehensive analysis. This instrumentation finds ubiquitous utility across diverse scientific domains such as chemistry, biochemistry, physics, and environmental science.

Light Source

In UV-Vis spectrometry, having a light source capable of emitting radiation across a wide range of wavelengths is fundamental. Typically, a xenon lamp is utilized as a high-intensity light source suitable for both UV and visible ranges. However, it's important to note that compared to tungsten and halogen lamps, xenon lamps are less stable and more costly (Tyson, 1984). Hence, UV-Vis spectrophotometers commonly incorporate two distinct lamps: a deuterium lamp for UV radiation and a halogen or tungsten lamp for visible light emission, ensuring comprehensive illumination coverage. These two lamps are employed to achieve optimal light intensity within the instrument. During the measurement of light intensity, the spectrometer must transition smoothly between the two light sources. A smoother transition occurs when this switchover takes place within the wavelength range of 300 to 350 nm, as both the visible and UV light sources emit comparable amounts of light at this wavelength.

Wavelength Selector

In order to optimize the spectral analysis of samples by harnessing the emitted wavelengths from the light source, meticulous wavelength selection is paramount for tailoring the analytical process to the characteristics of the analyte and sample under investigation (Jofre and Savio, 2023). Within the realm of UV-visible spectrometry, the cornerstone of wavelength selection lies in the utilization of the monochromator, esteemed for its proficiency in isolating light into precise wavelength bands. Radiation comprising a spectrum of wavelengths is directed into the monochromator via the entrance slit. Upon encountering the dispersing element at a predetermined angle, the incident beam undergoes dispersion, a pivotal phase in wavelength segregation. Typically, the monochromator incorporates a prism mechanism that facilitates the separation of the diverse wavelengths within the incident beam, thereby inducing non-linear dispersion. Consequently, only radiation of a singular color, aligned with a specific wavelength, is permitted to exit the monochromator, proceeding through subsequent stages or the exit slit for further analysis. The illumination source in UV-visible spectrophotometry typically involves a UV lamp, often a deuterium lamp for the UV range (190-400 nm), and a tungsten lamp for the visible range (400-800 nm). For more extensive spectral coverage across both UV and visible regions, sophisticated UV-Vis spectrophotometers may employ a xenon lamp (Liauw et al., 2010). The monochromator component serves as a pivotal element in this setup, effectively segregating polychromatic light into discrete wavelengths, thus facilitating precise wavelength selection for analytical purposes.

Prism or Grating

Monochromators can utilize prisms or diffraction gratings to disperse light into its constituent wavelengths.

Sample Compartment

This section holds the sample undergoing analysis and is designed to allow light passage through the sample. In the framework of a single-beam spectrophotometer, the entirety of radiation emitted from the light source traverses the sample as a unified beam. These instruments discern colour by assessing disparities in light source intensities prior to and subsequent to sample introduction (Aceto *et al.,* 2014). Typically, the wavelength range spans from 190 to 750 nm, though extensions up to 1100 nm are feasible. Conversely, in the configuration of a double-beam spectrophotometer, the radiation originating from the light source diverges into two separate beams: one transits through the sample while the other solely penetrates the reference material. Analogously, double-beam spectrophotometers offer a wavelength range spanning 190 to 1100 nm. Additionally, these instruments gauge absorbance in relation to wavelength or the ratio between sample and reference beam intensities.

Cuvette

Typically made of quartz or glass, the cuvette is a transparent container holding the liquid or solution under analysis.

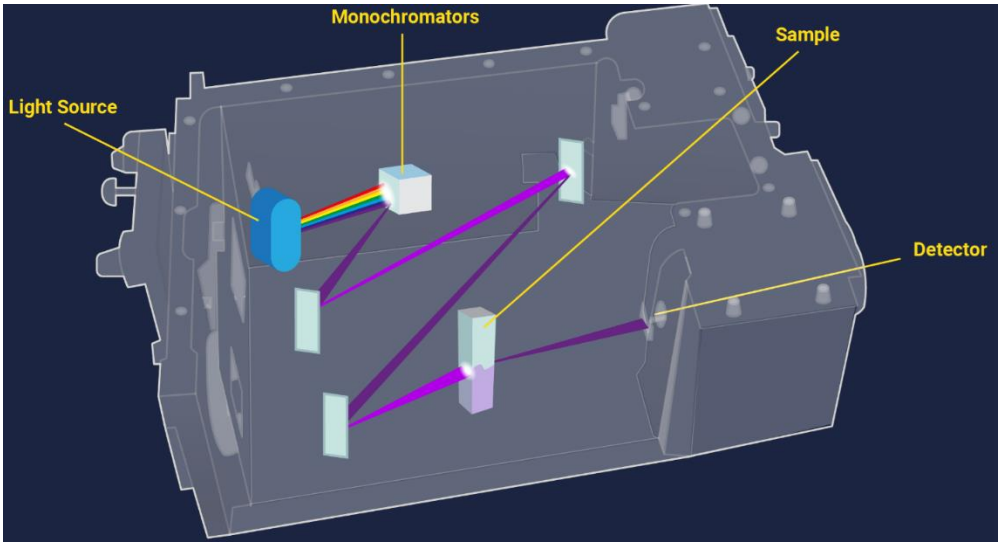


Figure 2: Schematic diagram of a cuvette-based UV-Vis spectroscopy system. ***Credit: Technology Networks***

Detector

The detector gauges the light intensity passing through the sample at a designated wavelength. Detectors in UV-visible spectroscopy are predicated upon photoelectric coatings or semiconductor materials, which facilitate the conversion of incident light emanating from the sample into an electrical signal or current. The magnitude of the current corresponds directly to the intensity of the incident light (Podborska *et al.,* 2020). These detectors are characterized by low noise levels and heightened sensitivity, thereby ensuring a linear response.

Furthermore, individual detectors exhibit distinct wavelength ranges and sensitivities tailored to specific analytical requirements. Ultimately, data acquisition typically involves the presentation of absorbance plotted against wavelength (measured in nanometers) within the UV and visible regions of the electromagnetic spectrum.

Photodiode Array Detector

Many modern UV-Vis spectrophotometers use a photodiode array detector, enabling simultaneous measurement at multiple wavelengths.

Wavelength Selector

This component chooses the desired light wavelength for analysis.

Rotating Grating or Prism

Users can select a specific wavelength by rotating the grating or prism. Amplifier and Signal Processor. The signal from the detector, usually weak, requires amplification and processing for accurate measurement.

Amplifier

Enhances the weak signal. Signal Processor: Converts the analog signal into a digital signal for further analysis. Display and Data Output:

Results, including absorbance values at different wavelengths, are presented on the instrument's screen.

Data Output

Findings can be exported to a computer or other data storage devices for subsequent analysis and documentation. Comprehending the various components and functions of a UV-Vis spectrophotometer is crucial for effective utilization in scientific applications, such as quantifying sample concentrations based on their absorption characteristics.

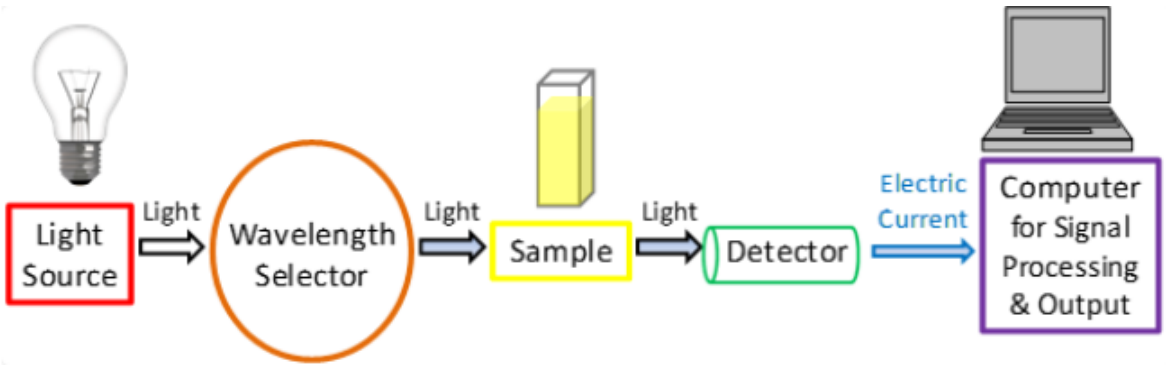


Figure 3: A simplified schematic of the main components in a UV-Vis spectrophotometer. ***Credit: Dr. Justin Tom.***

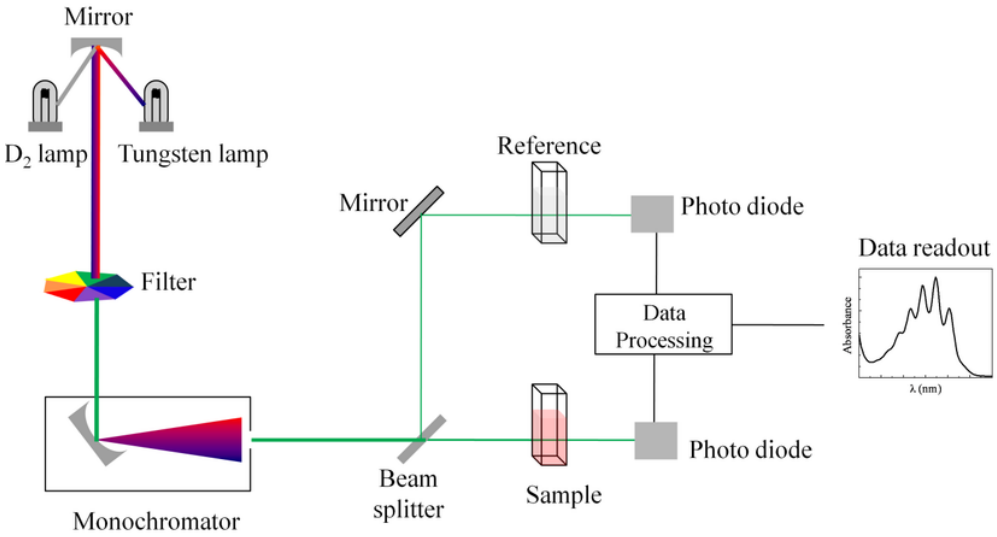


Figure 4: Set-up for UV-Vis Spectroscopy



Figure 5: UV-Vis Spectrophotometer

INSIGHTS FROM UV-VIS CHARACTERIZATION

In addition to chemical analysis, numerous physical methodologies are employed to ascertain purity and discern the composition of substances. Among these techniques, including the determination of melting point, refractive index, and density, Ultraviolet and Visible (UV/VIS) light spectroscopy holds considerable prominence across diverse sectors such as market segmentation, research domains, production, and quality control for substance classification and investigation. The UV/VIS spectrophotometer gauges light absorption by the sample when exposed to UV light, with each substance exhibiting distinctive light absorption properties. The degree of light absorption correlates with the substance concentration in the sample, facilitating quantitative analysis via UV/VIS spectrometry. Modern UV/Vis spectrophotometers offer rapid, facile, reliable, and precise results. This discourse delineates various applications of UV/Vis spectrophotometry. The UV-Visible spectrophotometer is designed to quantify and assess samples utilizing Ultraviolet-visible light spanning a wavelength range of 200nm to 900nm. In 1814, Fraunhofer Gesellschaft developed a spectroscope for sunlight measurement, subsequently discovering 574 dark fixed lines, commonly known as Fraunhofer lines. He

further refined his work in 1821 by developing a diffraction grating for light separation from the sun. Forty years later, David Rittenhouse devised the first artificial diffraction grating. In 1941, Arnold O Beckman introduced the inaugural commercial UV-Visible spectrophotometer for sample quantity and quality determination. The initial instrument utilized a quartz prism to disperse the light source (from the tungsten lamp) into absorption spectra, with a phototube serving as the detector in lieu of the modern photodiode. UV-Vis spectrophotometry measures both light intensity transmitted and sample absorption, reflecting sample properties. Although the optical principle of contemporary UV-Vis spectrophotometers has undergone minimal alteration, recent advancements in optical components have rendered modern UV-Vis spectrophotometers more resilient, expedient, adaptable, and compact. UV-Vis characterization of polyaniline thin films furnishes invaluable insights into various critical facets. Firstly, doping induces significant alterations in the electronic structure and conductivity of polyaniline, with UV-Vis spectroscopy serving as an essential tool for monitoring the doping process. Alterations in absorption spectra, such as the emergence of new peaks or shifts in peak positions, denote the incorporation of dopant molecules and subsequent modifications in the polymer's electronic milieu (Harisha et al., 2008). Secondly, the optical characteristics of polyaniline are intricately linked to the extent of π-conjugation along the polymer chain. UV-Vis spectroscopy aids in evaluating conjugation length by scrutinizing the energy of π-π* transitions, with extended conjugation lengths typically resulting in lower energy transitions and redshifts in absorption peaks (Li et al., 2014). Lastly, UV-Vis spectroscopy facilitates the identification of structural variations in polyaniline thin films, such as changes in chemical structure or morphology (Sun et al., 2015). Modifications in absorption peak intensity or broadening may signify defect formation, aggregation, or alterations in polymer conformation. It is imperative to underscore that UV-Vis spectroscopy remains a potent and indispensable analytical tool across diverse scientific disciplines. Its simplicity, versatility, and cost-effectiveness render it a preferred choice for research, analysis, and quality assurance endeavors. By furnishing pertinent insights into the electronic structure and composition of materials, UV-Vis spectroscopy continues to significantly propel advancements in both scientific inquiry and industrial applications.

LIMITATIONS OF UV-VIS SPECTROSCOPY

The constraints of UV-Vis spectroscopy encompass limited sensitivity for trace analysis, particularly for compounds with low absorption coefficients or at low concentrations (Li and Hur, 2017), potential challenges in distinguishing overlapping absorption bands in complex samples (Ríos-Reina and Azcarate 2022), and the method's inherent incapacity to provide detailed structural information, especially for intricate molecules or mixtures (Chen *et al.,* 2018). Additionally, UV-Vis spectroscopy may necessitate extensive sample preparation for certain samples and might not effectively probe specific chemical environments or interactions within a sample (Saleh, 2020). Its restricted wavelength range, ranging from the ultraviolet to the visible regions of the electromagnetic spectrum, limits its applicability for certain types of analysis (Munjanja and Sanganyado, 2015), and quantitative analysis can be hindered by factors such as sample matrix effects and instrumental drift (Jürgens et al., 2007). Furthermore, solvent effects, temperature sensitivity, and instrumental limitations, including stray light and detector constraints, pose additional hurdles in achieving accurate and precise measurements (McMahon, 2008; Upstone, 2000).

In their study published in 2011, Sridevi et al. described the synthesis process of polyaniline (PANI) nanocomposites using various dopants and characterized their optical properties using UV-Visible spectroscopy. The authors employed a method involving the addition of Aniline, Sulphuric acid, and dopant acid into a round bottom flask containing Millipore water, followed by stirring to form a homogeneous aqueous dispersion. Different dopants, including CSA and PTSA, were used, and the acid was added drop-wise with suitable concentration, followed by stirring in a magnetic stirrer. The polymerization process commenced with the slow addition of Auric acid, leading to a color change indicating the formation of PANI. The synthesized PANI was then washed with acetone and dried to obtain PANI powder. UV-Visible spectra of the PANI Emeraldine salt powder in N-methyl 2-pyrrolidone (NMP) were recorded using a Hitachi UV-Visible spectrometer. The spectra exhibited three characteristic absorbance peaks corresponding to π-π * transition, polaron-π * transition, and polaron-transition, indicating effective doping with primary and secondary dopants (Figure 6). Interestingly, PANI-Au nanocomposites did not show the surface plasmon resonance (SPR) absorption band of Au at 520 nm, suggesting deep incorporation of Au particles into the polymer chain.

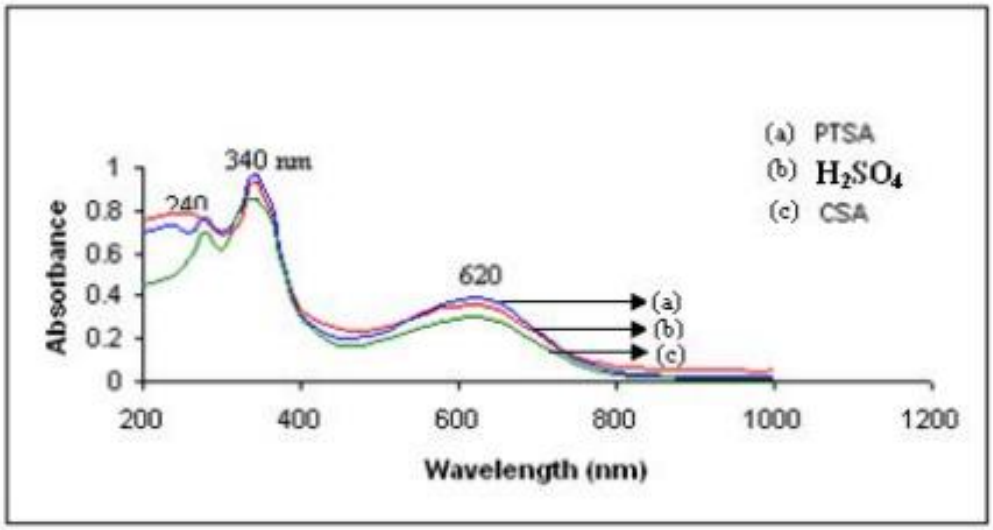


Figure 6: UV-Vis spectra of PANI/Au composites with different dopant acids.

This investigation yields valuable insights into the synthesis and optical characteristics of polyaniline (PANI) nanocomposites, thereby enriching the advancement of sophisticated materials across diverse applications. The implications drawn from the results are manifold. Initially, the detection of three distinctive absorbance peaks corresponding to specific transitions - specifically, π-π* transition, polaron-π* transition, and polaron-transition - denotes proficient doping with primary and secondary dopants. Such observations underscore a successful alteration of the material's electronic configuration, which holds significant relevance across a spectrum of applications, notably in the realms of electronic and optoelectronic devices. Moreover, the absence of the characteristic surface plasmon resonance (SPR) absorption band of gold (Au) at 520 nm within the PANI-Au nanocomposites suggests a profound integration of Au particles within the polymer matrix. This phenomenon indicates a robust interaction between the polymer framework and the Au nanoparticles, potentially culminating in heightened mechanical, electrical, or optical attributes. In aggregate, these

findings underscore the potential for customized material characteristics through adept doping strategies and nanoparticle integration, thereby paving the path for advancements in domains including sensors, catalysis, and nanoelectronics.

The study by Sironi *et al.* (2015) details the synthesis and characterization of polyaniline emeraldine base and P4ADPA, followed by the preparation of doped forms using salicylic and 5-sulfosalicylic acids. Polyaniline emeraldine base was synthesized through the reaction of aniline with HCl and $K_2S_2O_8$, resulting in a green solid with a 65% yield. P4ADPA was synthesized using 4-(aminodiphenyl) aniline, HCl, H_2O_2, and $FeCl_36H_2O$, yielding a dark blue-green solid with a 52% yield. The preparation of doped forms involved deprotonation, re-protonation with acids, and subsequent filtration and drying. UV-Vis spectroscopy characterized the samples, revealing characteristic peaks for benzenoid rings and azaquinoid moieties (Figure 7). The study highlighted differences in doping levels between salicylic and 5-sulfosalicylic acids, affecting film morphology and protonation degree. The research underscores the importance of these findings for understanding interactions between dopants and polymer chains as changes in absorption spectra can indirectly reflect variations in film morphology. For instance, variations in film thickness, roughness, or density can affect light absorption and result in shifts or broadening of absorption peaks (Ciambriello *et al.,* 2022).

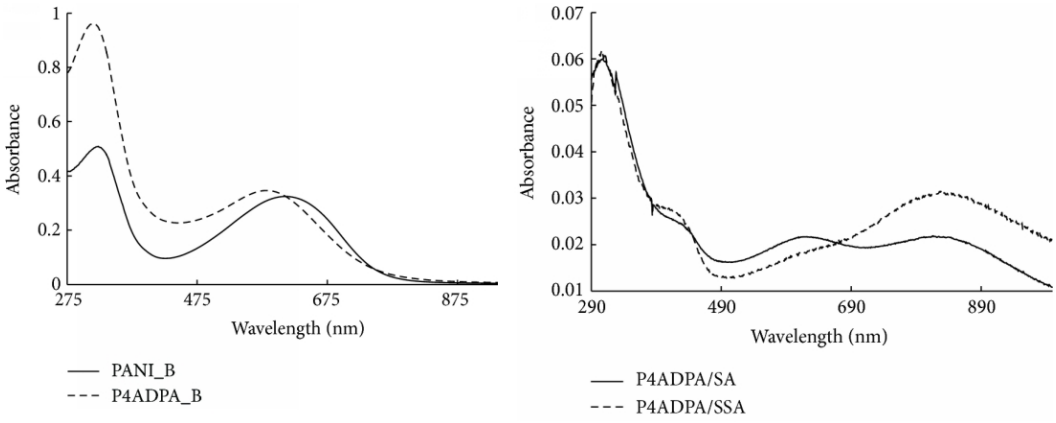


Figure 7: UV-Vis plot for PANI and its Nanocomposites

In another study, Solonaru and Grigoras (2017) synthesized reduced graphene oxide/polyaniline sulfonate (r-GO/PAnS) composites with different mass ratios using in-situ oxidative polymerization. Graphene oxide (GO) was obtained from graphite powder via the Hummers method and subsequently reduced to r-GO using hydrazine hydrate. The composites were prepared by dispersing r-GO in aqueous acidic solution, adding aniline sulfonate (AnS), and initiating polymerization with ammonium peroxydisulfate. The resulting nanocomposites, labelled as r-GO/PAnS-1, r-GO/PAnS-2, and r-GO/PAnS-3, were characterized by UV-Vis spectroscopy. The spectra exhibited characteristic peaks for electronic conjugation within r-GO and π-π* transitions in PAnS. Increasing PAnS content enhanced the visibility of UV absorption characteristic for PAnS as shown in Figure 8.

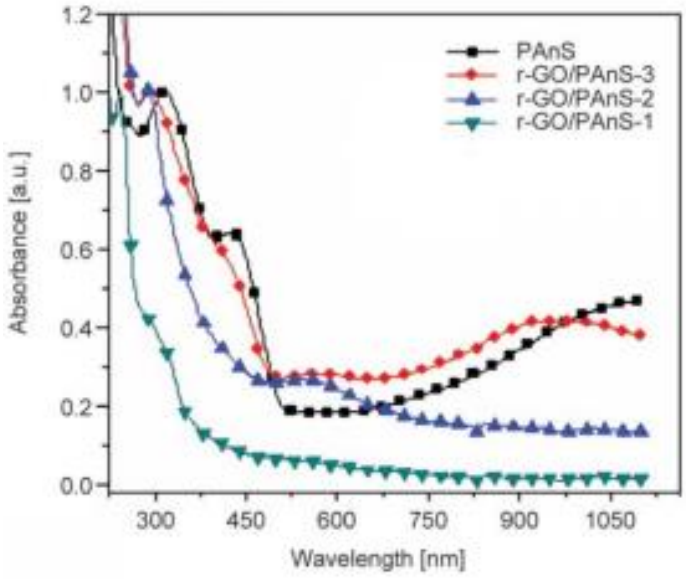


Figure 8: UV-Vis plot for PANI and its graphene nanocomposites

The investigation contributes valuable insights into the synthesis and characterization of r-GO/PAnS composites, which hold promise for diverse applications across multiple domains. Analysis via UV-Vis spectroscopy has yielded significant findings, with identified peaks indicative of electronic conjugation within r-GO and π-π* transitions within PAnS across the r-GO/PAnS-1, r-GO/PAnS-2, and r-GO/PAnS-3 composite variants. These outcomes validate the successful synthesis process and offer detailed elucidation of critical structural and optical attributes. The discernible presence of characteristic peaks serves to substantiate the composite formation, affirming the persistence of electronic characteristics within r-GO and the presence of extended conjugated systems within PAnS. Furthermore, the progressive enhancement in the discernibility of UV absorption features attributed to PAnS with escalating PAnS content underscores the direct influence exerted by PAnS concentration on optical characteristics. Such revelations bear considerable significance in the realm of material characterization, furnishing indispensable insights essential for the fine-tuning of composite compositions and the comprehensive comprehension of their behavior across an array of applications, notably within the realms of optoelectronics and sensor technologies.

Li et al. (2015) detailed the synthesis of FePOs and polyaniline (PANI) composites under varying conditions, exploring the impact of pH, temperature, molar ratios of H_2O_2: aniline, and reaction time. FePOs were prepared through a method involving $FeCl_2 \cdot 4H_2O$, NaH_2PO_2 55.H_2O, and polyvinylpyrrolidone (PVP), resulting in a product collected after centrifugation, washing, and drying. For PANI synthesis, PSS was dispersed in a buffer solution, and aniline monomer was added. The polymerization was catalyzed by FePOs and initiated by ammonium peroxydisulfate. UV-Vis spectra of PANI synthesized under different conditions revealed characteristic absorption bands at 430 nm and 800 nm, indicative of an intermediate redox state and the emeraldine state of PANI, respectively (Figure 9).

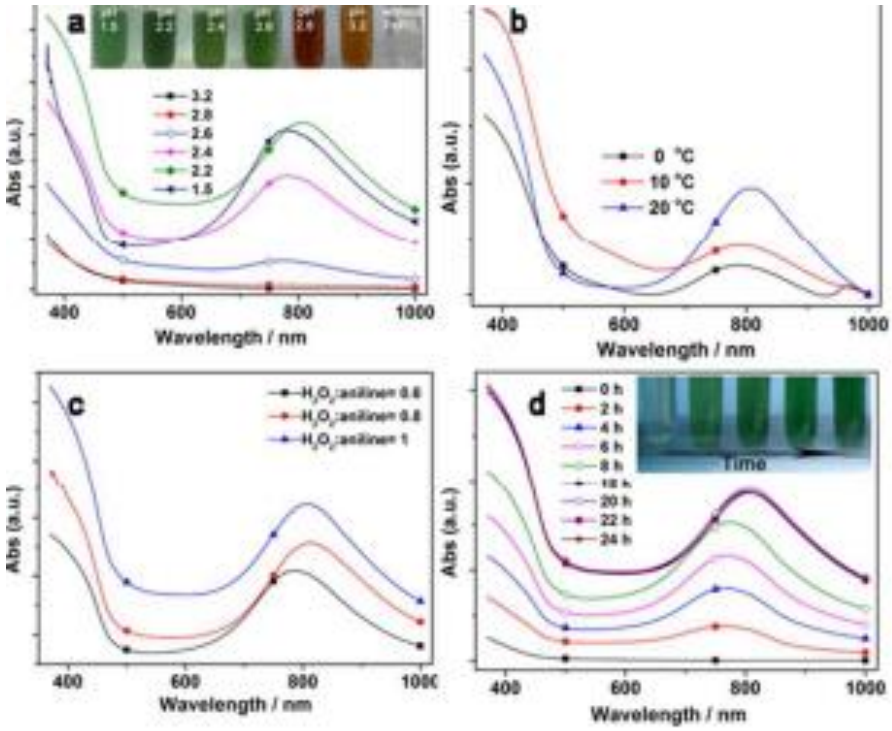


Figure 9: UV-Vis spectra of PANI synthesized under different conditions

The intensity of the latter was highest at pH 2.2, demonstrating pH dependency on the FePOs-catalyzed polymerization of PANI. The optimal pH was determined as 2.2, providing the highest conductivity and absorbance at 800 nm for the emeraldine form of PANI. FTIR spectra further supported the formation of the PSS and PANI complex. The research offers a comprehensive exploration of the synthesis conditions impacting the properties of FePOs-catalyzed polyaniline (PANI) composites. There may be various dimensions to these findings. Initially, the analysis of UV-Vis spectra pertaining to PANI synthesized under diverse conditions explained discernible absorption bands at 430 nm and 800 nm, indicative respectively of an intermediate redox state and the emeraldine state of PANI (Shah, 2007). This observation underscores the pivotal role played by synthesis parameters in delineating the oxidation state and structural attributes of PANI, thereby influencing its inherent properties and potential utility across various applications. Furthermore, the heightened intensity of the absorption band corresponding to the emeraldine state at pH 2.2 underscores the pH sensitivity inherent in the FePOs-catalyzed polymerization process of PANI. This underscores the criticality of pH modulation in achieving desired PANI configurations and functionalities. Additionally, the identification of the optimal pH value at 2.2, yielding the maximal conductivity and absorbance at 800 nm for the emeraldine form of PANI, offers valuable insights for refining PANI synthesis methodologies to optimize its efficacy across diverse applications. Moreover, the Fourier-transform infrared (FTIR) spectra serve to complement the UV-Vis findings by affirming the formation of the complex between polystyrene sulfonate (PSS) and PANI, thereby enhancing the comprehension of the structural attributes of the synthesized PANI under varying conditions. In summary, these outcomes contribute significantly to an enhanced understanding of synthesis parameters and their impact on the structural and optical characteristics of PANI, thereby facilitating the tailored development of PANI materials for a broad spectrum of technological applications.

In their quest to studying the optical properties of PANI and some cellulose derivatives, Geng *et al*. (1999) undertook an investigation employing three distinct Polyethylene Glycol Methylether (PEGME) derivatives, specifically DEGME, PEGME-350, and PEGME-550, denoted by numerical indices representing the molecular weights of the respective PEGME constituents. These derivatives served as initial substrates for the synthesis of corresponding phosphonic acids (PA), identified as PADEG, PA-350, and PA-550. The synthetic process entailed the introduction of 0.3 mol PEGME in 50 ml benzene into a dispersion containing 0.1 mol P_2O_5, followed by heating and agitation. Subsequent to the elimination of residual P_2O_5 and solvent, a colourless and transparent liquid amalgam of mono- and bi-hydroxyl acids was procured, maintaining a molar ratio of 1:1. The approximated average molecular weights of the dopants were discerned to be 253, 596, and 896 g mol^{-1} for PA-DEG, PA-350, and PA-550, correspondingly. The formulations for the fabrication of films were established through the amalgamation of PANI–PA (molar ratio 1:0.5), PEG or PVP, and distilled water, achieving concentrations of 10.0, 5.0, and 5.0 g per 100 ml, sequentially. The composite solution was methodically formulated by gradual incorporation of PANI/PA solution into the PEG or PVP solution under consistent stirring. Subsequent to the casting of films onto glass substrates and air drying at ambient conditions, a vacuum drying procedure was implemented at 40°C for 24 hours preceding the subsequent characterization steps. The UV-VIS spectroscopic analysis conducted on the resultant films manifested distinctive spectra (Figure 10).

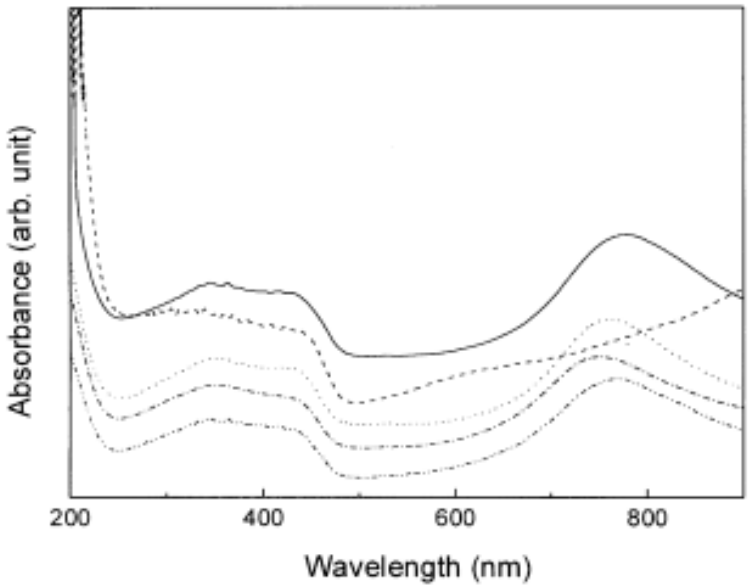


Figure 10: UV-Vis spectroscopic graph of PANI and PANI-PA

Films derived from varied solvent solutions exhibited characteristic peaks at 325, 430, and 750–800 nm, indicative of doped PANI. Of particular note, the film derived from an NMP solution exhibited a distinct shoulder at approximately 620 nm, accompanied by absorption bands at 325, 430, and surpassing 900 nm, signifying incomplete doping of PANI. This incomplete doping phenomenon was attributed to the feeble basicity of NMP and the subdued acidity of the dopant, aligning with prior observations delineated by Geng et al (1997). The implications of the results are significant. The UV-Vis spectroscopic analysis conducted on the

resulting films revealed distinct spectra, with films derived from different solvent solutions displaying characteristic peaks at 325, 430, and 750–800 nm, indicative of doped polyaniline (PANI). Notably, the film derived from an NMP solution exhibited a discernible shoulder at approximately 620 nm, alongside absorption bands at 325, 430, and extending beyond 900 nm. This observation suggests incomplete doping of PANI in the film derived from the NMP solution (Mohammad, 2001). Incomplete doping can have implications for the material's conductivity, optical properties, and stability, affecting its suitability for various applications. Additionally, understanding the factors influencing doping efficiency, such as solvent choice, is crucial for optimizing the synthesis process and tailoring PAni films for specific applications, such as in sensors, electronic devices, or energy storage systems.

The study conducted by Hussin et al. (2017) focused on the synthesis and characterization of water-soluble polyaniline (PANI) and its derivatives with cellulose compounds. The authors utilized various chemicals, including Aniline (Ani), methylcellulose (MC), hydroxypropyl cellulose (HPC), hydroxypropyl methylcellulose (HPMC), and ammonium persulfate (APS) obtained from Sigma-Aldrich, as well as Hydrochloric acid (HCl, 37%) from Lab Scan Sdn. Bhd. All chemicals were used without further purification. The synthesis process involved the use of a dialysis tube with a 14kDa molecular weight cut-off (MWCO) to create water-soluble PANI through chemical oxidation polymerization. Aniline served as the monomer, cellulose derivatives acted as steric stabilizers, 1M HCl functioned as a dopant, and APS served as an initiator. The procedure included dissolving 0.5 g of MC in 1M HCl at 80 °C, followed by the careful addition of Ani at 0 °C. After stirring for 3 hours, APS was slowly introduced to initiate polymerization, which continued for 24 hours.

The resulting polymer was purified through dialysis with 1M HCl as the dialysate for 6 hours to remove unreacted monomers and oligomers. The same procedure was repeated for PANI-HPC and PAni-HPMC with equivalent amounts of HPC and HPMC. The electrical conducting behaviour of PAni-cellulose derivatives was analyzed through UV-Vis spectroscopy in the wavelength range of 300 nm to 900 nm. The UV-Vis spectra revealed three essential absorption bands for PAni, including a free-carrier tail above 800 nm (indicating π–polaron transition band), an absorption band around 450 nm (polaron- π* transition band caused by protonation of PAni backbone), and an absorption band around 350 nm (π- π* electron transition within the benzenoid ring). The study interpreted the results by comparing the UV-Vis spectra of water-soluble PAni-cellulose derivatives. The disappearance of the absorption band around 350 nm in the complexes suggested interaction between PAni chains and water-soluble polymers (Figure 11).

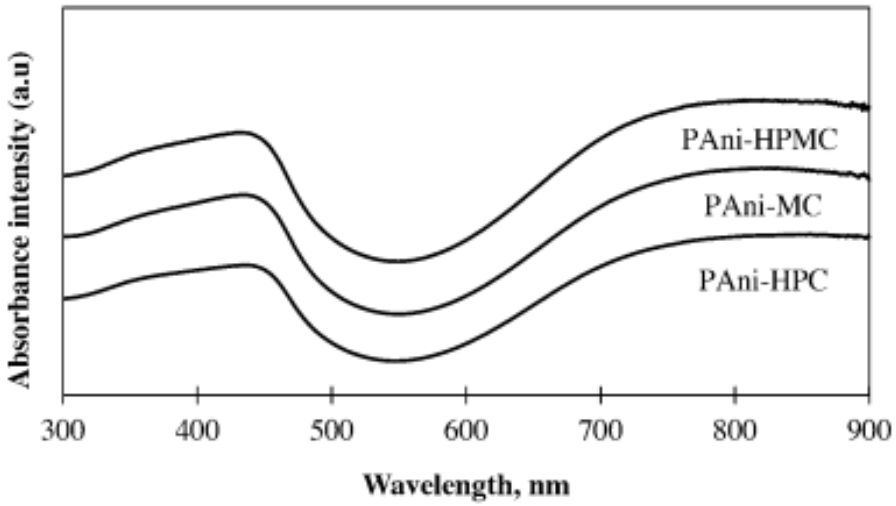


Figure 11: UV-Vis graph on PANI and its cellulose derivatives

Additionally, the cellulose derivatives' rigid and expanded chain structures, facilitated by hydrogen bonding with amine groups on PANI chains, were discussed as factors contributing to the extended conformation of the complexes. The absorption bands around 800 nm, showing a free-carrier tail, indicated the possibility of extended conformation in the near-infrared (NIR) region, leading to higher conductivity. The study concluded that water-soluble PANI-cellulose derivatives indeed exhibit an extended conformation, as evidenced by their UV-Vis spectra. The ramifications of the outcomes are profound and varied. The UV-Vis spectroscopic examination unveiled three pivotal absorption bands delineating the characteristics of polyaniline (PANI): an extension beyond 800 nm indicative of a π–polaron transition band, an absorption band centered around 450 nm attributed to the polaron-π* transition band arising from PANI backbone protonation, and an absorption band approximately at 350 nm representing the π-π* electron transition within the benzenoid ring. The explication of the findings entailed a comparative analysis of UV-Vis spectra encompassing water-soluble PANI-cellulose derivatives. The absence of the absorption band near 350 nm within the complexes implied an interplay between PANI chains and water-soluble polymers. Furthermore, the discourse delved into the rigid and expanded chain structures of cellulose derivatives, facilitated by hydrogen bonding with amine groups on PANI chains, as elements fostering the elongated conformation of the complexes. The detection of absorption bands nearing 800 nm, denoting a free-carrier tail, hinted at the prospect of an elongated conformation within the near-infrared (NIR) spectrum, potentially auguring heightened conductivity. These revelations elucidate the intricate molecular interplays within PANI-cellulose complexes, furnishing insights into their structural attributes and conductivity traits, pivotal for their applicability across diverse domains such as sensor technology, electronics, and energy storage.

Alam et al. (2013) conducted a synthesis of polyaniline (PANI) in its emeraldine salt form utilizing the redox process involving aniline, ammonium peroxy disulfate (APS) as an oxidant, and hydrochloric acid (HCl). Subsequently, the PANI salt underwent conversion to emeraldine base upon treatment with ammonium hydroxide solution. The PANI-SnO_2 nanocomposite was synthesized via the co-precipitation method, where tin chloride dihydrate ($SnCl_2 \cdot 4H_2O$) was dissolved in distilled water followed by the addition of ammonium solution under vigorous

stirring. PANI (5-10 wt%) was then introduced to the solution, resulting in the precipitation of the composite, which was subsequently washed and dried. Characterization of the PANI-SnO_2 nanocomposite was performed using UV-Vis spectroscopy, revealing a red shift in absorption transition indicative of successful interaction between the metal nanoparticles and the polymer chain. Furthermore, the synthesis process of the PANI-SnO_2 nanocomposite via in situ chemical polymerization of aniline with ammonium persulphate as the oxidizing agent yielded a well-crystalline structure with a uniform distribution of SnO_2 nanoparticles within the PANI matrix. Notably, strong chemical interaction between PANI and SnO_2 nanoparticles was observed, contributing to the observed red shift in UV-Vis spectra. This successful synthesis approach via the co-precipitation method holds promise for the development of advanced materials endowed with enhanced properties. The well-crystalline structure and homogeneous dispersion of SnO2 nanoparticles within the PANI matrix are indicative of successful incorporation and dispersion of the nanoparticles, potentially leading to improved material performance (Faisal et al., 2020). The observed strong chemical interaction between PANI and SnO_2 nanoparticles, as evidenced by UV-Vis spectroscopy, suggests the formation of a stable composite material with promising applications across various fields such as optoelectronics, sensors, and energy devices. The successful synthesis and characterization of the PANI-SnO_2 nanocomposite offer valuable insights into the design and development of novel hybrid materials tailored for advanced technological applications. UV-Vis spectroscopy emerges as a crucial analytical tool for assessing the optical properties of materials, including their absorption and transmission characteristics in the ultraviolet and visible regions. This technique facilitates the elucidation of electronic transitions and band gaps, providing valuable information regarding the electronic structure and energy levels of materials.

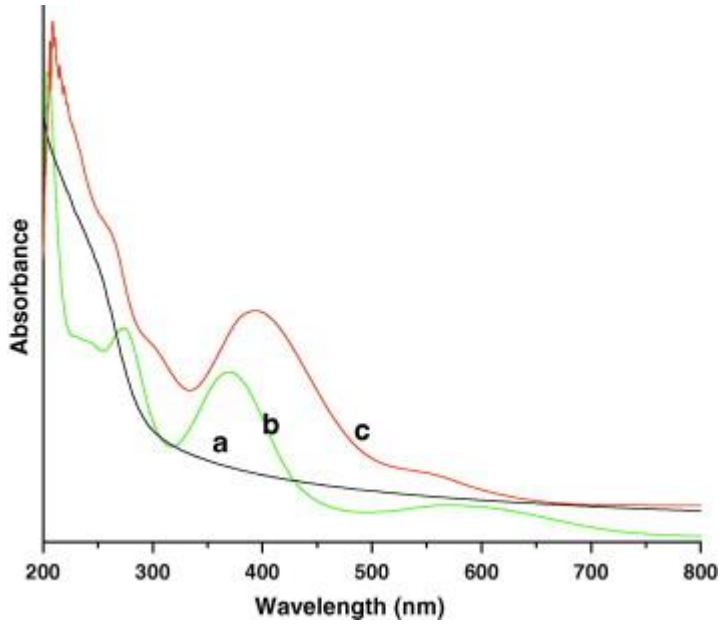


Figure 12: UV–Vis spectra of (a) SnO_2, (b) PANI and (c) PANI/SnO_2 nanocomposite.

Moreover, UV-Vis spectroscopy enables the investigation of interactions between different components in nanocomposite materials, such as PANI and SnO_2 nanoparticles, through the observation of absorption spectra and associated band shifts. The red shift observed in the UV-

Vis spectra of the PANI-SnO_2 nanocomposite signifies successful interaction between the metal nanoparticles and the polymer chain, underscoring the formation of a composite material with modified optical properties. Figure 12 presents the UV–Vis spectra of SnO_2, PANI, and the PANI/SnO_2 nanocomposite, visually illustrating the spectral characteristics of each component and the resultant composite material. Overall, UV-Vis spectroscopy emerges as a valuable tool for characterizing the optical behavior and potential applications of nanocomposite materials, particularly in optoelectronic, sensing, and energy-related devices.

Choudhury's (2009) comprehensive research delved into the experimental synthesis and characterization of polyaniline/silver (PANI/Ag) nanocomposites. The synthesis process involved the procurement of analytical grade aniline monomer, silver nitrate ($AgNO_3$), and sodium borohydride ($NaBH_4$) from Sigma–Aldrich (USA), while reagent grade ammonium peroxodisulphate ($(NH_4)_2S_2O_8$), hydrochloric acid (HCl), and ethanol were acquired from Merck India Ltd. The synthesis of nanosized silver particles commenced with the chemical reduction of $AgNO_3$ using $NaBH_4$ in deionized (DI) water. Different mole percentages of $AgNO_3$ were dissolved in deionized water to prepare silver nitrate solutions, which were subsequently subjected to reduction by the gradual addition of the aqueous solution of $NaBH_4$. This process yielded yellowish-red colloidal silver nanoparticles, with dynamic light scattering (DLS) and transmission electron microscopy (TEM) revealing average particle diameters of approximately 3 nm and 5 nm, respectively. PANI/Ag nanocomposites were synthesized through an in-situ chemical oxidation polymerization process. Aniline-hydrochloride was introduced into the previously prepared Ag nanoparticles colloid, followed by the addition of the aqueous solution of $(NH_4)_2S_2O_8$.

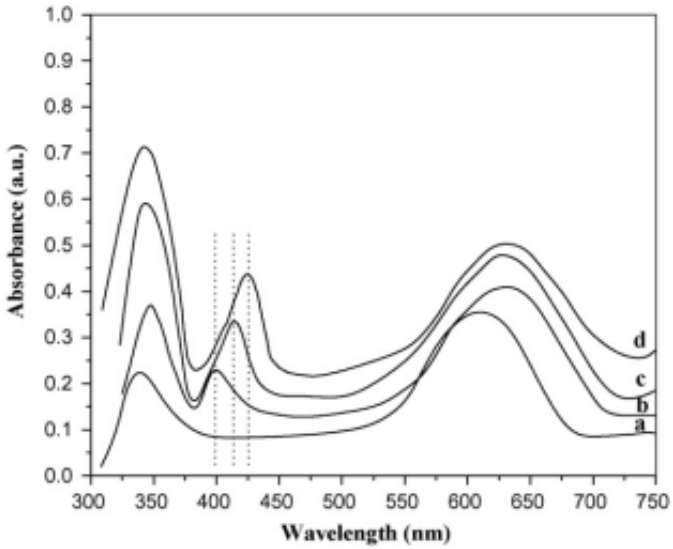


Figure. 13: UV–vis absorption spectra of pure PANI (a) and PANI/Ag nanocomposites prepared with Ag concentrations of 0.5 mol% (b), 1.5 mol% (c) and 2.5 mol% (d).

The resulting mixture underwent a reaction under constant stirring at low temperature for 12 hours, after which the product was filtered, washed, and dried. Pure PANI was synthesized using the same chemical polymerization method in the absence of silver colloid. For UV–vis spectroscopic analysis, both pure PANI and PANI/Ag nanocomposite samples in powder form

were dispersed in ethanol, and their absorption spectra were recorded using a Shimadzu UV1601 spectrophotometer with a spectral resolution of 2 nm. The UV–vis absorption spectra of pure PANI exhibited characteristic peaks (Figure 13) at approximately 342 nm and 624 nm, corresponding to π-π* and n-π* transitions, consistent with previous studies (Kulkarni and Viswanath, 2004; Kohut-Svelko et al., 2005).

Conversely, the UV–Vis spectra of PANI/Ag nanocomposites displayed similar absorption bands but with a slight red shift, attributed to the strong interaction between polyaniline and silver. Notably, PANI/Ag nanocomposites exhibited a sharp peak between 400 and 425 nm, indicative of the surface plasmon resonance absorption of electrons in the conducting silver bands (Zhang et al., 2002). The UV–Vis spectroscopic analysis conducted on both pure polyaniline (PANI) and PANI/silver (Ag) nanocomposite samples dispersed in ethanol revealed significant findings. The presence of characteristic absorption peaks at approximately 342 nm and 624 nm in the UV–Vis spectra of pure PANI, consistent with π-π* and n-π* transitions as reported in previous studies, validates the purity and structural integrity of the PANI samples. Conversely, a slight red shift observed in the PANI/Ag nanocomposite spectra indicates a strong interaction between PANI and silver, likely attributable to physical adsorption or chemical interactions (Choudhury, 2009). Notably, the emergence of a sharp peak between 400 and 425 nm in the PANI/Ag nanocomposite spectra signifies surface plasmon resonance (SPR) absorption, suggestive of the presence of Ag nanoparticles within the PANI matrix. These results not only confirm the successful synthesis of PANI/Ag nanocomposites but also imply their potential utility in various applications such as optoelectronics and sensing owing to their unique structural and optical properties.

The study conducted by Zheng et al. (2021) was characterized by a thorough investigation into the synthesis and characterization of polyaniline (PANI) nanostructures, shedding light on the crucial factors influencing its conductivity and structural properties. The experimental procedures and analytical techniques employed were meticulously outlined, offering valuable insights for researchers in the field. High-quality reagents were sourced from reputable suppliers, ensuring the reliability of the experimental setup. Aniline and HCl, procured from QReC Sdn. Bhd. and APS from Sigma-Aldrich (M) Sdn Bhd, were utilized without further purification. Deionized water from UTM's analysis lab maintained the purity of the solvent. The utilization of the BILON-1200Y ultrasonic reactor facilitated the chemical oxidative polymerization of PANI nanostructures, following a methodology adapted from Mohsin et al. (2019). Notably, all materials were utilized as received, underscoring the efficiency of the experimental process. The synthesis protocol involved meticulous control of reaction parameters, including temperature and sonication time, crucial for achieving desired PANI nanostructures. Initially, different molar ratios of APS/aniline were explored under fixed HCl concentration, leading to the identification of optimized conditions. Subsequent experimentation involved varying HCl concentration while maintaining the optimized APS/aniline molar ratio, enabling a comprehensive understanding of its impact on PANI conductivity. Characterization techniques, including UV–Vis spectroscopy, provided valuable insights into the structural evolution of PANI nanostructures. Analysis of UV–Vis spectra revealed distinct absorption bands corresponding to various structural motifs within PANI chains. Notably, the correlation between absorption band intensity and conductivity elucidated the doping level of PANI, corroborating findings from previous studies by Li et al. (2006), Qiu

et al. (2017), and Geethalakshmi et al. (2015). Furthermore, Zheng et al. (2021) effectively correlated experimental results with established literature, reinforcing the validity of their findings. Through meticulous experimentation and analysis, the authors have contributed significantly to the understanding of PANI synthesis and characterization, paving the way for advancements in the field. Through meticulous analysis of UV–Vis spectra, the study identified distinct absorption bands corresponding to different structural motifs within PANI chains (Figure 14).

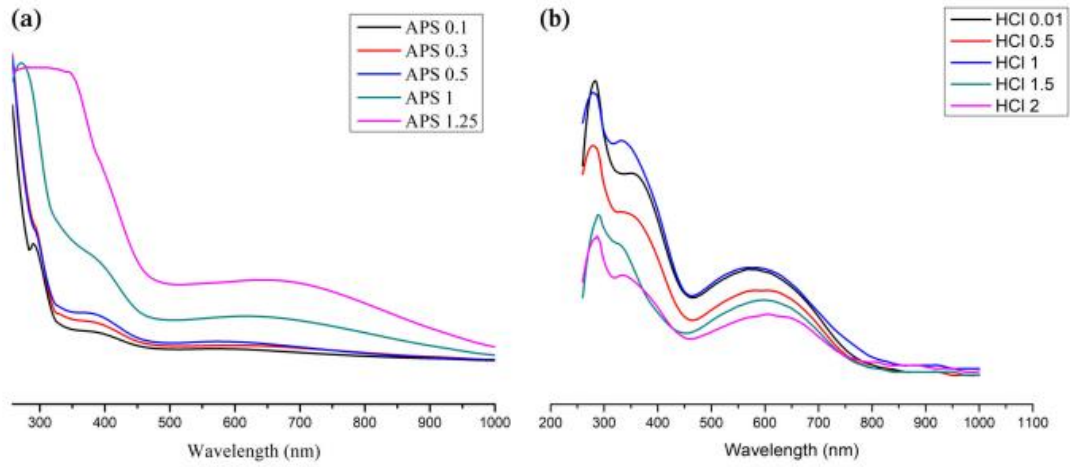


Figure 14: UV–Vis spectra of polymerization of polyaniline synthesized by varying (a)APS/aniline molar ratio (b) HCl concentration.

This provided crucial insights into the structural evolution of PANI nanostructures, essential for tailoring their properties for various applications. Moreover, the study revealed a correlation between absorption band intensity and conductivity, elucidating the doping level of PANI and emphasizing the importance of understanding its structural features in relation to its electrical properties. The validation of these findings through comparison with established literature enhanced their credibility, reinforcing the existing body of knowledge on PANI synthesis and characterization. Overall, Zheng et al.'s research contributes significantly to advancing the understanding and application of PANI in the field of conductive polymer materials.

SUMMARY

Polyaniline (PANI) has garnered significant interest in diverse scientific fields due to its versatile electrical, optical, and chemical properties. The utilization of PANI thin films and nano-composites in applications such as sensors, optoelectronic devices, and energy storage systems underscores the necessity of comprehending their optical behavior for enhanced functionality. UV-Vis spectroscopy emerges as a crucial analytical tool for investigating PANI materials, offering profound insights into their electronic structure and interactions. PANI, as a conducting polymer, exhibits intriguing characteristics resulting from the delocalization of π-electrons along its backbone, modifiable through chemical doping or structural alterations. Fabrication methods like spin-coating, dip-coating, or electrochemical deposition provide controlled environments for exploring PANI properties. UV-Vis spectroscopy facilitates the examination of electronic transitions within PANI thin films, aiding in the identification of

characteristic peaks and deductions about structural and electronic modifications. Despite its utility, UV-Vis spectroscopy has limitations such as limited sensitivity for trace analysis and challenges in distinguishing overlapping absorption bands. Several studies have explored the synthesis and characterization of PANI and its composites using UV-Vis spectroscopy, providing valuable insights into their optical properties and potential applications in various domains.

CONCLUSION

The multifaceted properties of polyaniline (PANI) have garnered significant attention in various scientific fields, with its applications ranging from sensors to energy storage systems. Understanding the optical behavior of PANI thin films and nano-composites is crucial for enhancing their functionality, with UV-Vis spectroscopy serving as a pivotal analytical technique in this regard. By delving into electronic transitions within PANI materials, UV-Vis spectroscopy offers profound insights into their structural and electronic modifications. Looking ahead, the future prospects of PANI research intertwined with UV-Vis spectroscopy are promising. Continued advancements in characterization techniques and instrumentation will enable researchers to delve deeper into the intricate properties of PANI materials. Furthermore, the exploration of PANI nano-composites and their interactions with various nanofillers opens up avenues for tailoring their optical properties for specific applications, such as optoelectronic devices and sensors. Moreover, as demonstrated by recent studies, the synthesis and characterization of PANI-based materials using UV-Vis spectroscopy provide valuable insights into their structural evolution and performance. Further research efforts focusing on optimizing synthesis parameters, understanding dopant-polymer interactions, and exploring novel applications will undoubtedly drive the field forward. In essence, the combination of PANI and UV-Vis spectroscopy holds immense potential for addressing current challenges and innovating future technologies across diverse domains. As researchers continue to unravel the intricacies of these materials and their optical properties, the possibilities for advancement and application are boundless.

Conflict of Interest: We, the authors, declare no conflicts of interest that could influence this study. We have no financial or personal relationships affecting outcomes.

Funding: NA

References

1. Aceto, M., Agostino, A., Fenoglio, G., Idone, A., Gulmini, M., Picollo, M., ... & Delaney, J. K. (2014). Characterisation of colourants on illuminated manuscripts by portable fibre optic UV-visible-NIR reflectance spectrophotometry. *Analytical methods*, *6*(5), 1488-1500.

2. Alam, M., Ansari, A. A., Shaik, M. R., & Alandis, N. M. (2013). Optical and electrical conducting properties of Polyaniline/Tin oxide nanocomposite. *Arabian Journal of Chemistry*, *6*(3), 341-345.

3. Banerjee, J., Dutta, K., Kader, M. A., & Nayak, S. K. (2019). An overview on the recent developments in polyaniline-based supercapacitors. *Polymers for Advanced Technologies*, *30*(8), 1902-1921.

4. Beygisangchin, M., Baghdadi, A. H., Kamarudin, S. K., Rashid, S. A., Jakmunee, J., & Shaari, N. (2024). Recent progress in polyaniline and its composites; Synthesis, properties, and applications. *European Polymer Journal*, 112948.

5. Blasco-Gomez, F., Bosch-Reig, F., Campins-Falco, P., Molins-Legua, C., & Herráez-Hernández, R. (2000). H-point curve isolation method for coupled liquid chromatography and UV− visible spectrophotometry. *Analytical Chemistry*, *72*(11), 2559-2565.

6. Chen, W., Qian, C., Zhou, K. G., & Yu, H. Q. (2018). Molecular spectroscopic characterization of membrane fouling: a critical review. *Chem*, *4*(7), 1492-1509.

7. Choudhury, A. (2009). Polyaniline/silver nanocomposites: Dielectric properties and ethanol vapour sensitivity. *Sensors and Actuators B: Chemical*, *138*(1), 318-325.

8. Ciambriello, L., Cavaliere, E., & Gavioli, L. (2022). Influence of roughness, porosity and grain morphology on the optical properties of ultrathin Ag films. *Applied Surface Science*, *576*, 151885.

9. Faisal, M., Rashed, M. A., Abdullah, M. M., Harraz, F. A., Jalalah, M., & Al-Assiri, M. S. (2020). Efficient hydrazine electrochemical sensor based on PANI doped mesoporous SrTiO3 nanocomposite modified glassy carbon electrode. *Journal of Electroanalytical Chemistry*, *879*, 114805.

10. Förster, H. (2004). UV/vis spectroscopy. *Characterization I: -/-*, 337-426.

11. Geethalakshmi, D., Muthukumarasamy, N., & Balasundaraprabhu, R. (2015). [Title of the article]. *Optik*, *125*(3), 1307.

12. Geng, Y. H., Li, J., Jing, X. B., & Wang, F. S. (1997). Synth Met, 77, 97.

13. Geng, Y. H., Sun, Z. C., Li, J., Jing, X. B., Wang, X. H., & Wang, F. S. (1999). Water soluble polyaniline and its blend films prepared by aqueous solution casting. *Polymer*, *40*(20), 5723-5727.

14. Harisha, A., Ravindrachary, V., Bhajantri, R. F., Sanjeev, G., Poojary, B., Dutta, D., & Pujari, P. K. (2008). Electron irradiation induced microstructural modifications in BaCl2 doped PVA: A positron annihilation study. *Polymer degradation and stability*, *93*(8), 1554-1563.

15. Hussin, H., Gan, S. N., Mohamad, S., & Phang, S. W. (2017). Synthesis of water-soluble polyaniline by using different types of cellulose derivatives. *Polymers and Polymer Composites*, *25*(7), 515-520.

16. Ibanez, J. G., Rincón, M. E., Gutierrez-Granados, S., Chahma, M. H., Jaramillo-Quintero, O. A., & Frontana-Uribe, B. A. (2018). Conducting polymers in the fields of energy, environmental remediation, and chemical–chiral sensors. *Chemical reviews*, *118*(9), 4731-4816.

17. Jofre, F. C., & Savio, M. (2023). Infrared radiation: A sustainable and promising sample preparation alternative for inorganic analysis. *TrAC Trends in Analytical Chemistry*, 117469.

18. Jürgens, J., Paama, L., & Leito, I. (2007). The uncertainty of UV–Vis spectrophotometric and FAAS analysis for the determination of iron in pharmaceutical products. *Accreditation and quality assurance*, *12*, 593-601.

19. Kohut-Svelko, N., Reynaud, S., & Francois, J. (2005). Synthesis and characterization of polyaniline prepared in the presence of nonionic surfactants in an aqueous dispersion. *Synthetic Metals, 150*, 107–114.

20. Kulkarni, M. V., Viswanath, A. K. (2004). Comparative studies of chemically synthesized polyaniline and poly(o-toluidine) doped with p-toluene sulphonic acid. *European Polymer Journal, 40*(3), 379–384.

21. Li, G., Pang, S., Xie, G., Wang, Z., Peng, H., & Zhang, Z. (2006). [Title of the article]. *Polymer*, *47*(5), 1456.

22. Li, L., Liang, K., Hua, Z., Zou, M., Chen, K., & Wang, W. (2015). A green route to water-soluble polyaniline for photothermal therapy catalyzed by iron phosphates peroxidase mimic. *Polymer Chemistry*, *6*(12), 2290-2296.

23. Li, P., & Hur, J. (2017). Utilization of UV-Vis spectroscopy and related data analyses for dissolved organic matter (DOM) studies: A review. *Critical Reviews in Environmental Science and Technology*, *47*(3), 131-154.

24. Li, Y., Dandu, N., Liu, R., Li, Z., Kilina, S., & Sun, W. (2014). Effects of extended π-conjugation in phenanthroline (N∧ N) and phenylpyridine (C∧ N) ligands on the photophysics and reverse saturable absorption of cationic heteroleptic iridium (III) complexes. *The Journal of Physical Chemistry C*, *118*(12), 6372-6384.

25. Liauw, M. A., Baylor, L. C., & O'Rourke, P. E. (2010). UV-Visible Spectroscopy for On-Line Analysis. *Process analytical technology: Spectroscopic tools and implementation strategies for the chemical and pharmaceutical industries*, 81-106.

26. McMahon, G. (2008). *Analytical instrumentation: a guide to laboratory, portable and miniaturized instruments*. John Wiley & Sons.

27. Mohammad, F. (2001). Stability of electrically conducting polymers. In *Handbook of advanced electronic and photonic materials and devices* (pp. 321-350). Academic Press.

28. Mohsin, M. E. A., Shrivastava, N. K., Basar, N., & Arsad, A. (2019). Front Mater. 6(1).

29. Munjanja, B., & Sanganyado, E. (2015). UV-Visible Absorption, Fluorescence, and Chemiluminescence Spectroscopy. *Handbook of Food Analysis*, *31*, 572-583.

30. Pan, J., Cha, T. G., Li, F., Chen, H., Bragg, N. A., & Choi, J. H. (2017). Visible/near-infrared sub diffraction imaging reveals the stochastic nature of DNA walkers. *Science advances*, *3*(1), e1601600.

31. Penner, M. H. (2017). Basic principles of spectroscopy. *Food analysis*, 79-88.

32. Podborska, A., Suchecki, M., Mech, K., Marzec, M., Pilarczyk, K., & Szaciłowski, K. (2020). Light intensity-induced photocurrent switching effect. *Nature Communications*, *11*(1), 854.

33. Purcell, D. K. (2013). *UV-visible microscope spectrophotometric polarization and dichroism with increased discrimination power in forensic analysis*. City University of New York.

34. Qiu, B., Li, Z., Wang, X., Li, X., & Zhang, J. (2017). [Title of the article]. *Polym. Sci. Part A Polym. Chem.*, *55*(11), 3357.

35. Ríos-Reina, R., & Azcarate, S. M. (2022). How chemometrics revives the UV-Vis spectroscopy applications as an analytical sensor for spectralprint (nontargeted) analysis. *Chemosensors*, *11*(1), 8.

36. Saleh, T. A. (2020). Trends in the sample preparation and analysis of nanomaterials as environmental contaminants. *Trends in Environmental Analytical Chemistry*, *28*, e00101.

37. Shah, A. U. H. A. (2007). *Electrochemical synthesis and spectroelectrochemical characterization of conducting copolymers of aniline and o-aminophenol* (Doctoral dissertation, Chemnitz, Techn. Univ., Diss., 2007).

38. Sironi, A., Marinotto, D., Riccardi, C., Zanini, S., Guerrini, E., Della Pina, C., & Falletta, E. (2015). Effect of salicylic acid and 5-sulfosalicylic acid on UV-Vis spectroscopic characteristics, morphology, and contact angles of spin coated polyaniline and poly (4-aminodiphenylaniline) thin films. *Journal of Spectroscopy*, *2015*.

39. Skoog, D. A., Holler, F. J., & Nieman, T. A. (1998). Principles of instrumental analysis: Douglas A. *Skoog, F. James Holler, Timothy A. Nieman. 5th ed. Belmont (CA): Brooks/Cole*.

40. Smith, N. A., Krebs, J. F., & Hebden, A. S. (2015). *UV-vis spectroscopy as a tool for safeguards; instrumentation installation and fundamental data collection* (No. ANL/NE-15/7). Argonne National Lab. (ANL), Argonne, IL (United States).

41. Solonaru, A. M., & Grigoras, M. (2017). Water-soluble polyaniline/graphene composites as materials for energy storage applications. *Express Polymer Letters*, *11*(2), 127

42. Sridevi, V., Malathi, S., & Devi, C. S. (2011). Synthesis and characterization of polyaniline/gold nanocomposites. *Chem. Sci. J*, *26*(1).

43. Sun, G., Zhang, X., Rappich, J., & Hinrichs, K. (2015). In situ infrared ellipsometric monitoring of the growth process of polyaniline thin films and doping with poly (4-styrenesulfonate). *Applied Surface Science*, *344*, 181-187.

44. Sykes, P. (1986). *A guidebook to mechanism in organic chemistry*. Pearson Education India.

45. Tolbin, A. Y., Pushkarev, V. E., Tomilova, L. G., & Zefirov, N. S. (2017). Threshold concentration in the nonlinear absorbance law. *Physical Chemistry Chemical Physics*, *19*(20), 12953-12958.

46. Tyson, J. F. (1984). Light sources and optical components. In *Practical Absorption Spectrometry: Ultraviolet Spectrometry Group* (pp. 36-47). Dordrecht: Springer Netherlands.

47. Upstone, S. L. (2000). Ultraviolet/visible light absorption spectrophotometry in clinical chemistry. *Encyclopedia of analytical chemistry*, 1699-1714.

48. Zhang, J. H., Li, X. L., Liu, K., Cui, Z. C., Zhang, G., Zhao, B., & Yang, B. (2002). Thin films of Ag nanoparticles prepared from the reduction of AgI nanoparticles in self-assembled films. *Journal of Colloid and Interface Science, 255*, 115–118.

49. Zhao, Z., Zhang, H., Lam, J. W., & Tang, B. Z. (2020). Aggregation-induced emission: new vistas at the aggregate level. *Angewandte Chemie International Edition*, *59*(25), 9888-9907.

50. Zheng, X., Ali Mohsin, M. E., Arsad, A., & Hassan, A. (2021). Polymerization of polyaniline under various concentrations of ammonium peroxydisulfate and hydrochloric acid by ultrasonic irradiation. *Journal of Applied Polymer Science*, *138*(27), 50637.